

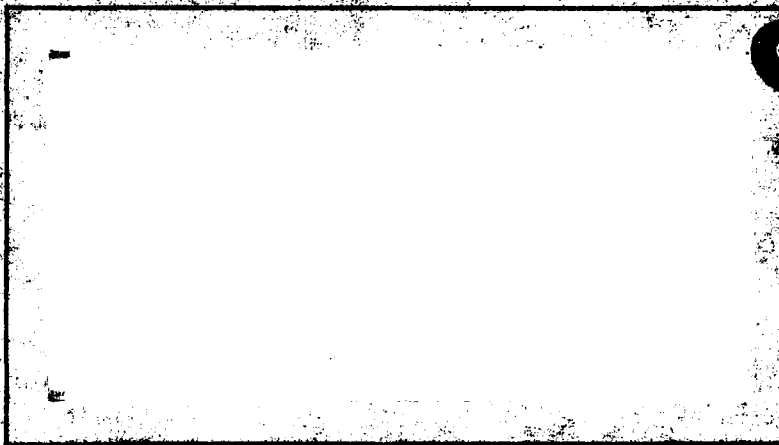


AD 1094791

# AIR FORCE INSTITUTE OF TECHNOLOGY



AIR UNIVERSITY  
UNITED STATES AIR FORCE



DTIC  
SELECTED  
FEB 9 1981

## SCHOOL OF ENGINEERING

WRIGHT-PATTERSON AIR FORCE BASE, OHIO

DEC FILE COPY



14

AFIT/GEO/PH/80-2

12

1 Dec 74

1 Director, AFOSR



6

RETURN WAVE ANALYSIS IN  
A THERMALLY BLOOMED MEDIUM.

THESIS

AFIT/GEO/PH/80-2/ Michael T. Baker  
1st Lt USAF

12/67

APPROVED FOR PUBLIC RELEASE AFR 190-17.

Approved for public release; distribution unlimited

23 JAN 1981

*Laurel A Lampela*

LAUREL A. LAMPELA, 2Lt, USAF  
Deputy Director, Public Affairs  
Air Force Office of Technology (ATC)  
Wright-Patterson AFB, OH 45433

012225 SW

81 2 09 019

AFIT/GEO/PH/80-2

RETURN WAVE ANALYSIS IN A  
THERMALLY BLOOMED MEDIUM

THESIS

Presented to the Faculty of the School of Engineering  
of the Air Force Institute of Technology  
Air University  
in Partial Fulfillment of the  
Requirements for the Degree of  
Master of Science

by

Michael T. Baker, B. S.

1st Lt                      USAF

Graduate Electro-Optics

December 1980

Approved for public release; distribution unlimited.

Preface

The purpose of this study was to analyze how a reflected wave is disturbed as it propagates from a reflecting surface to a receiver plane via a thermally bloomed medium. Previous studies on this subject have been done. However, this study incorporates more sophisticated models for the thermal blooming and ray propagation portions of the analysis.

Along with the return wave analysis, this report includes a computer program developed to perform a geometrical ray trace through the thermally bloomed medium. The program is thoroughly documented and can be easily adapted to any blooming model. In its present form, the program is adapted for use with the Air Force Weapons Laboratory blooming model known as PROPMD.

I would like to thank my advisor, Major John Erkkila of the Air Force Institute of Technology, for his timely guidance that was so essential to the progress of this study. Thanks also goes to Major William MacInnes of the Air Force Weapons Laboratory for his help with the PROPMD computer code. And finally, I want to express my gratitude to my family for their consideration and support throughout the entire study.

Michael T. Baker

Accession For
NTIS GRA&I
DTIC TAB
Unannounced
Justification
By
Distribution/
Availability
and
Special
A

## Contents

	Page
Preface .....	ii
List of Figures .....	iv
Abstract .....	v
I. Introduction .....	1
Background .....	1
Problem .....	3
Assumptions .....	4
Development .....	5
II. Computer Program Development .....	6
PROPMD Data .....	6
Design Intent .....	6
Index Screen Locations .....	7
Index Interpolation .....	8
Optical Path Difference (OPD)in Receiver Plane .....	8
Strehl Ratio .....	9
Receiver Plane Masking .....	10
Program Verification .....	10
III. Analysis.....	12
Receiver Plane Contours.....	12
Strehl Ratio .....	13
Location of Blooming Effects .....	13
IV. Results .....	14
Ray Refraction and Tilt .....	14
Strehl Calculations .....	19
Location of Blooming Effects .....	21
V. Conclusions and Recommendations .....	27
Bibliography .....	30
Appendix A: Luneburg's 3-D Refraction .....	31
Appendix B: PROPMD - A Thermal Blooming Model .....	35
Appendix C: Program Source Listings for Trace and Data.	41
Vita .....	58

## List Of Figures

<u>Figure</u>	<u>Page</u>
1. Heated Medium Resembles Negative Lens.....	1
2. Refractive Index Profile With Crosswind.....	2
3. Geometry of OPD.....	9
4. OPD Contour Plot for Power of 25,000 Watts.....	16
5. OPD Contour Plot for Power of 75,000 Watts.....	17
6. OPD Contour Plot for Power of 100,000 Watts.....	18
7. Strehl Ratio vs Aperture Radius.....	20
8. Strehl Ratio vs Screens Skipped (P = 25,000 W).....	23
9. Strehl Ratio vs Screens Skipped (P = 75,000 W).....	24
10. Strehl Ratio vs Screens Skipped (P = 100,000 W).....	25
11. Geometrical Representation.....	32
12. Phase Screen Locations in PROPMD.....	37

Abstract

A computer code was developed to perform a geometrical ray trace of a light ray from a target plane to a receiver plane via a thermally bloomed medium. Thermal blooming was modeled using an Air Force Weapons Laboratory computer code called PROPMD.

Ray traces were done for various degrees of thermal blooming, and Strehl ratio calculations were made for each situation. Also, contour plots of the ray optical path deviations across the receiver plane were made.

Results showed that a ray's direction of propagation was virtually unaffected by refraction. Disturbance of the ray was due totally to the effect of thermal blooming on the optical path length of the ray. In severe blooming situations, calculated Strehl ratios were less than 0.1. However, limiting the size of the receiver optics to something less than the size of a high-energy beam grid led to improved Strehl ratios.

# RETURN WAVE ANALYSIS IN A THERMALLY BLOOMED MEDIUM

## I INTRODUCTION

### Background

Propagation of a high power laser beam through an absorbing medium has been shown to be a nonlinear process. As the beam propagates, some of its energy is absorbed by the medium, and this absorption induces temperature changes within the medium. The temperature changes affect the density of the medium which in turn affect the refractive index  $n$  through the relationship

$$n_1 = [n_0 - 1] \rho_1 / \rho_0 \quad (1)$$

where  $n_0$  is the refractive index of the quiescent medium,  $\rho_0$  is its quiescent gas density,  $n_1$  is the index change, and  $\rho_1$  is the density change. The relationship between temperature and density is such that as temperature increases, density (and refractive index) decreases. If we consider the irradiance profile of a Gaussian beam where the center of the beam is the hottest area, the medium resembles a negative lens (see Figure 1) and the beam is defocused (Ref 1:27-19).

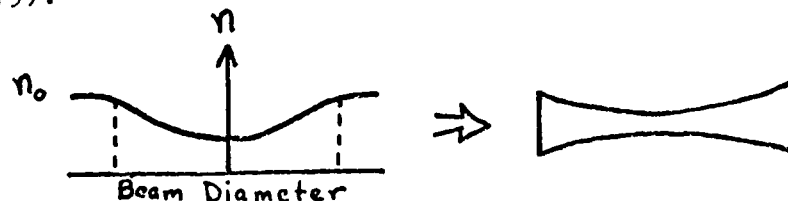


Figure 1. Heated Medium Resembles Negative Lens

When a crosswind (wind traveling in a direction perpendicular to that of the laser beam) is present, heating across the beam is redistributed and the refractive index profile for the beam changes (see Figure 2). This change is due to the cooling effect that the wind has on the beam. As parcels of air within the beam are heated up, they are swept out of the beam by the wind. Since the downwind portion of the beam sees less of a cooling effect than the upwind portion, the index profile resembles that shown in Figure 2. In addition to causing the beam to diverge slightly, this profile also causes the beam to bend into the wind.

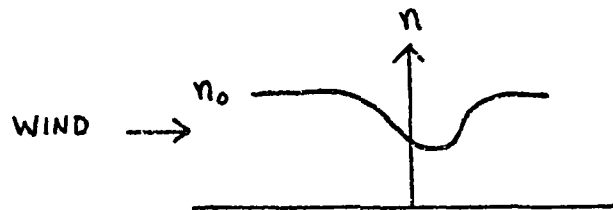


Figure 2. Refractive Index Profile with Crosswind

From the standpoint of classical geometrical optics, if the refractive index of any point within the beam can be determined, then a Snell's Law analysis of a light ray traveling inside the beam can be performed. Furthermore, a calculation of the optical path length (OPL) can be made for any particular ray, the OPL being the integral of the refractive index along the ray path.

With the help of an Air Force Weapons Laboratory (AFWL) computer code called PROPMD and the basic assumptions listed later in this section, a geometrical optics analysis is possible.

An analysis of this nature is of interest to AFWL since low power lasers (serving as tracking lasers) share the same aperture as and travel colinearly with high power laser beams. If it were possible for the laser operator to form an image of the target by using the return wave reflections from the target, then the laser operator could determine not only if he was hitting the target but also what specific area of the target he was hitting.

#### Problem

The problem investigated in this study is the analysis in the receiver plane of a wave that has emanated from a point in the target plane, and traveled through a thermally bloomed medium to the receiver.

The analysis does not include the effects of diffraction on the propagation. Furthermore, the analysis is related only to the return wave prior to its entering the receiver imaging optics.

### Assumptions

It must be emphasized that the accuracy of all results of this research are dependent upon the overall accuracy of the PROPMD computer code calculations. Based on an analysis of PROPMD calculations and on certain properties of the PROPMD code, the following assumptions are made:

a. The value of the index of refraction for any particular x-y coordinate point in an index screen (an array of index values in a plane perpendicular to the direction of ray propagation) remains constant for that x-y position from a z coordinate point midway between that index screen and the preceding index screen to a z coordinate point midway between that index screen and the next successive index screen.

b. Based on the first assumption, refraction takes place only at points in the plane midway between any two index screens.

c. The index of refraction value used in calculating the OPL between any two successive index screens is (through linear interpolation) the average value of the two indices.

The basic assumptions of the PROMPD code are:

a. The beam has been on long enough to establish a steady-state irradiance distribution.

b. The heat transfer process within the beam is instantaneous, thus producing instantaneous temperature changes that translate to instantaneous refractive index

changes.

c. The high-energy beam has an unperturbed irradiance profile that is Gaussian in shape.

d. The medium through which the beam passes is free of turbulence and is flowing at a constant velocity that is much less than the speed of sound.

The wavelength of the high-energy beam used in this study is 10.6 micrometers.

No consideration is given to rays that reach the edge of the beam grid prior to reaching the receiver plane. The rays are allowed to leave the grid and are not included in calculations made in the receiver plane.

#### Development

The design of the ray trace algorithm is presented in chapter II. Special attention is given to certain portions of the computer code that are special adaptations of otherwise general knowledge.

In Chapter III, the methods of analysis are discussed. The various results of the analysis are compared in Chapter IV, and the conclusions and recommendations are presented in Chapter V.

## II COMPUTER CODE DEVELOPMENT

The most difficult and time consuming portion of this study has been the development and validation of the computer code that performs the geometrical ray trace. However, before the ray trace program could be used, certain other data were needed.

### PROPMD Data

Early in this research effort, PROPMD was studied in order to understand the mechanics of the program and where certain information is calculated within the program. A discussion of how PROPMD functions, the changes made to it, and a sample listing of the input parameters used can be found in Appendix B.

### Design Intent

The ray trace program called TRACE is designed to propagate a ray from a specified position in the target plane to the receiver plane through a medium whose refractive index varies as a function of position. As the ray propagates, its initial direction and velocity are affected by the variations in density and refractive index from point to point. This requires a three-dimensional (3-D) Snell's Law refraction (see Appendix A for detailed development) of the ray at points along the propagation path where refractive index changes are significant.

Additionally, a cumulative calculation of the OPL is needed with

$$OPL = \sum_i \int_{IS_{i-1}}^{IS_i} n(r) dr \quad (2)$$

where

$n$  = refractive index

$r$  = the vector between the two index screens

$IS_i$  =  $i$ th index screen

As stated in the previous chapter, the linear interpolation between planes gives

$$n(r) = [n_{i-1} + n_i] / 2 = \bar{n}_i \quad (3)$$

Thus, the form of the OPL equation

$$OPL = \sum_i \int_{IS_{i-1}}^{IS_i} \bar{n}_i dr = \sum_i \bar{n}_i r_i \quad (4)$$

is used for all calculations within TRACE.

#### Index Screen Locations

TRACE is designed to be given the location of the index screens along the propagation path. As each index screen location is read, the appropriate midplane locations are determined for later calculations of refraction and OPL.

### Index Interpolation

As a ray propagates to a new midplane, its angle of incidence (with respect to the surface normal of the midplane) is calculated as well as its new x-y coordinates. The next step is then to determine the value of  $n$  at that x-y coordinate in the index plane. This determination of the value is based on a linear interpolation subroutine called ANDEX. ANDEX reads in a square matrix representing the index distribution across the index plane. Based on the spacing between array values (grid spacing value determined by PROPM), a linear interpolation is performed. Since the coordinate system of PROPM is opposite to that of the ray trace, the interpolation begins in the upper right-hand corner of the index grid where  $n(1,1)$  is located.

### Optical Path Difference (OPD) In Receiver Plane

In order to determine what changes the image in the receiver plane has undergone, it is necessary to determine how much the phase front of the actual image wave differs from that of a perfectly spherical wave that has propagated the same range distance through an unperturbed medium. This ideal value of OPL is subtracted from the cumulative OPL value for each ray. To find the true OPD within the receiver plane for each ray,  $\delta$  (see Figure 3) is found

using

$$\delta = \sqrt{x^2 + y^2 + z^2} - z \quad (5)$$

The final OPD is found using

$$\text{OPD} = \text{OPL} - \delta n_f \quad (6)$$

where  $n_f$  is the final refractive index for any particular ray (Ref 3:197). Figure 3 assumes that  $n_o$  is the final index value and that  $\delta$  is small compared to  $z$ .

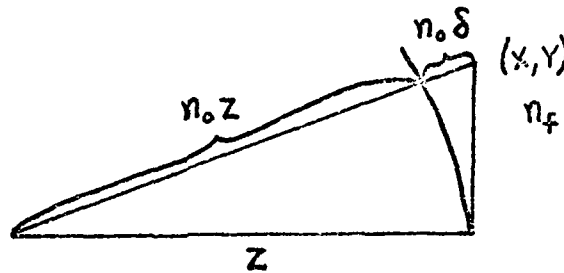


Figure 3. Geometry of OPD Calculation.

Strehl Ratio (Refs 4:1513;5:460-464)

If the variations in OPD across the receiver plane are small enough (on the order of 0.5 wavelengths or less), then the Strehl ratio (a ratio of the peak intensity in the focal plane of a disturbed wave front to the peak intensity in the focal plane of an ideal undisturbed wave front) can be

approximated by

$$\text{Strehl} = 1 - \left(\frac{2\pi}{\lambda}\right)^2 \left[ \overline{\text{OPD}^2} - \overline{\text{OPD}}^2 \right] \quad (7)$$

where

$\overline{\text{OPD}^2}$  = the average of the square of OPD

$\overline{\text{OPD}}^2$  = the square of the average OPD

$\lambda$  = the wavelength

#### Receiver Plane Masking

In order to analyze how the Strehl ratio varies as the size of the receiver plane being analyzed is varied, a parameter call MASK is input to TRACE. This parameter determines what radius with respect to the center of the receiver plane is analyzed in the Strehl ratio calculations.

#### Program Verification

The validity of the refraction and propagation portions of TRACE were verified by simulating a propagation through three phase screens. The index values at each plane were constants. The output values of TRACE were checked against hand calculations and found to be consistent.

The interpolation portion of the program was verified by inputting a 4x4 index array to TRACE. The previously determined indices for selected points on the index grid were then compared to the interpolated values from TRACE.

The comparison showed complete agreement between the two values.

### III ANALYSIS

Since there are so many parameters in the thermal blooming model that can be varied, all parameters except power, number of screens, and crosswind velocity are kept constant (see Appendix B for a complete listing of PROPMD parameters). All analysis is for a range of 1000 meters, and the power levels studied are 100, 10,000, 25,000, 50,000, 75,000, and 100,000 watts. Analysis of these power levels is done for crosswind velocities of 2.57 and 144. meters per second for both 5 and 10 screens.

Due to the problems with computer access and job turn around, the size of the index array at each index screen is limited to 64 x 64. This array size directly affects the distance between array points, and, ultimately, the resolution of index changes.

#### Receiver Plane Contours

As discussed earlier, a high-energy laser beam will bend into the wind when a crosswind is present, and the downwind portion of the beam will have a lower refractive index than the upwind portion. One will then see a symmetry transverse to the crosswind direction when contour plots of the OPD in the receiver plane are plotted for waves originating from an on-axis point in the target plane.

### Strehl Ratio

The Strehl ratio is the standard of measurement for return wave quality in this study. Since the Strehl ratio is directly related to phases and phases are directly related to OPD's, the Strehl ratio calculation can be made using the final OPD values. Furthermore, it might be possible to determine if the return wave over a certain area of the receiver plane is less affected than that of another area. Part of the analysis deals with a masking of the receiver plane such that the Strehl calculations include only those values of OPD falling within a previously specified radius of the center of the receiver plane.

### Location Of Blooming Effects

In an attempt to determine at what point along the propagation path the thermal blooming has its greatest effect on the return wave, various numbers of index screens are skipped before refraction takes place. Up to and including the screen skipped, the OPL calculation uses  $n_0$  so as to simulate propagation through an ambient medium. The Strehl ratios with the various screens skipped can then be compared to determine which screens contribute the most to OPD.

## IV RESULTS

The findings being discussed in this section are the result of analyzing data generated through the following process:

1. Executing the PROPMD program using a selected combination of input parameters.
2. Executing the DATA program to translate the PROPMD program output into the required sequence of index screens.
3. Executing the TRACE program to calculate the final x-y positions and OPD values for the input values of ray origin and launch angle representing a bundle of rays directed from the target back to the receiver (TRACE uses the index screen information to do the refraction and OPD calculations).
4. Drawing contour plots and making Strehl ratio calculations using the OPD values for those rays that have propagated to the receiver plane.

The following discussion attempts to explain the findings in each major area of analysis. Particularly significant results are highlighted, and comparisons are made of data differences associated with the variation of PROPMD input parameters.

### Ray Refraction and Tilt

In this portion of the analysis, a contour plot of OPD

values for each ray with respect to that ray's final x-y position in the receiver plane was made. As expected, these plots showed the OPD to be symmetric with respect to the crosswind flow direction. As can be seen in Figures 4, 5, and 6; the contours are similar with only the distance between the OPD contour lines changing. From a total variation in OPD of 0.5 waves (waves =  $OPD/\lambda$ ) at 25,000 watts, we see a variation of 2.0 waves at 100,000 watts.

When comparing each ray's final x-y position to the projected position for that same ray had it traveled through a homogeneous medium, we find that there is no deviation of the rays. This comparison implies that, for the beam powers and ranges studied herein, ray refraction effects are negligible.

However, there is a nearly linear variation of OPD versus distance in the direction of wind flow. A linear variation of phase is equivalent to tilt of the wavefront, and phase can be directly related to OPD. The tilt is related to the bending into the wind of the high energy beam that disturbed the medium. Wavefronts propagating through this disturbed medium also tend to bend. This bending causes returning wavefronts to be tilted with respect to the receiver plane.

The refraction technique used in this study does not correct the ray direction to account for the presence of wavefront tilt, so a rough calculation was done to estimate

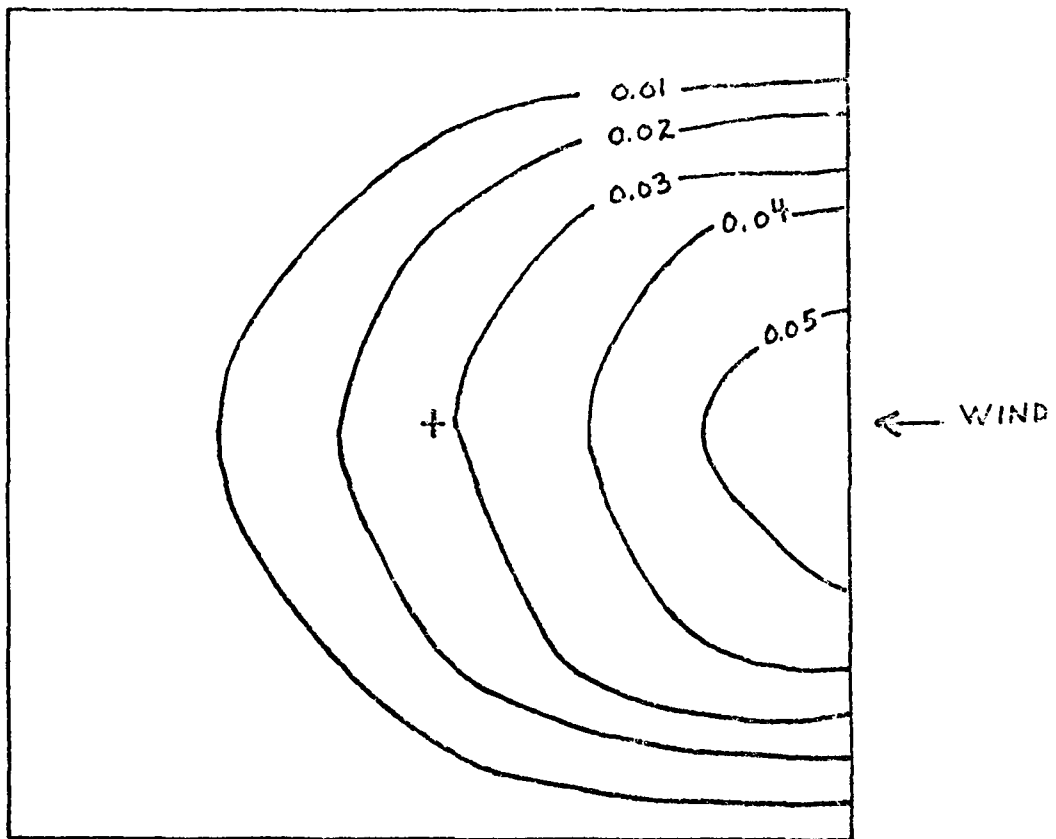


Figure 4. OPD Contour Plot for Power of 25,000 W( $10^{-4}$ m)

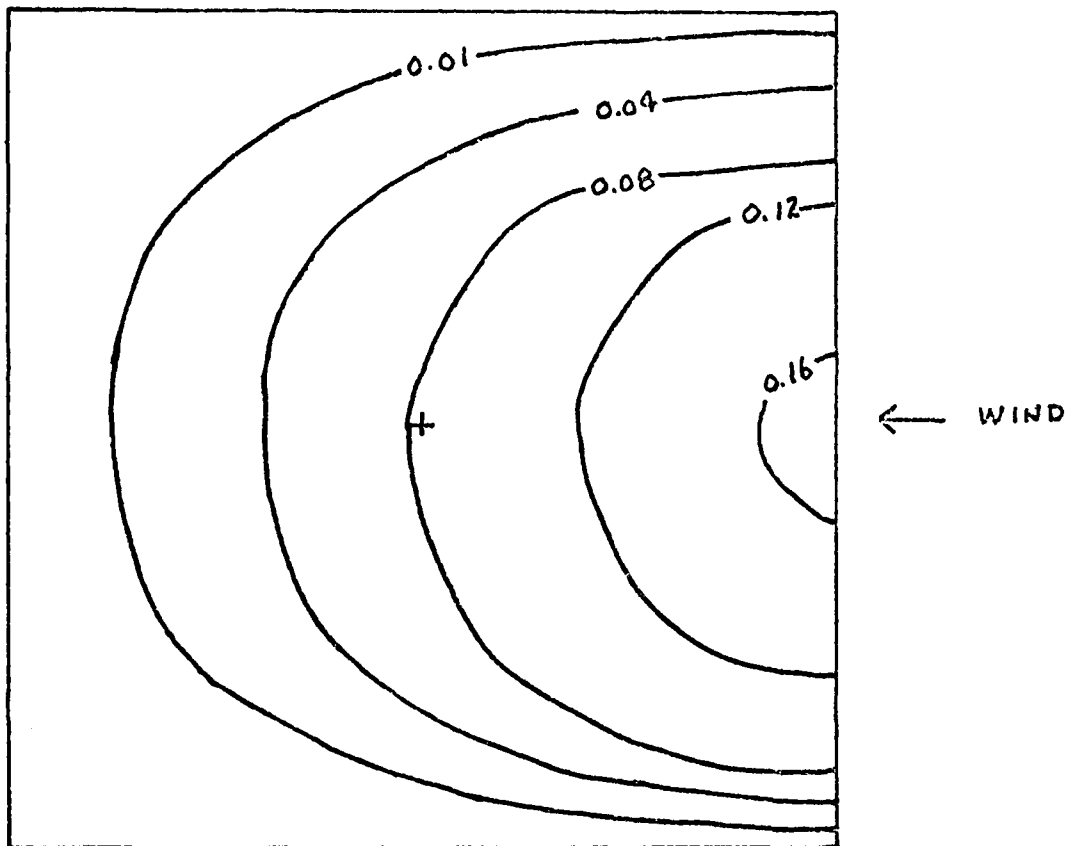


Figure 5. OPD Contour Plot for Power of  $75,000 \text{ W}(10^{-4} \text{ m})$

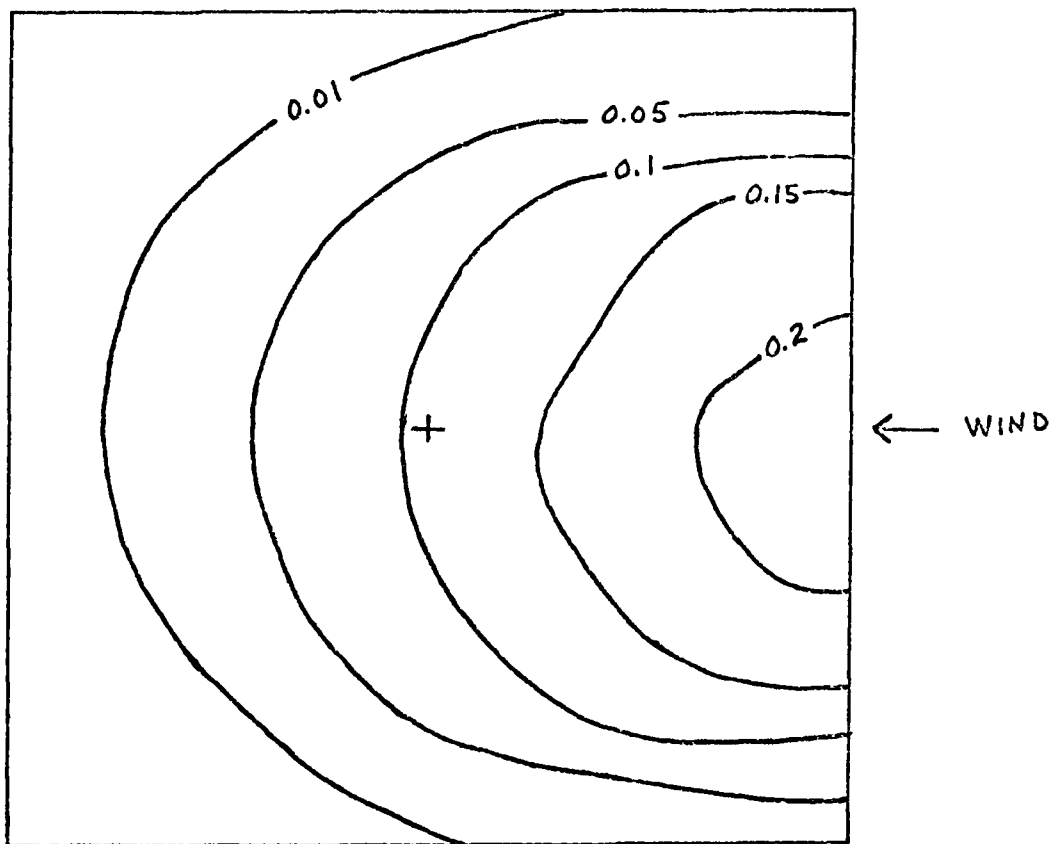


Figure 6. OPD Contour Plot for Power of 100,000 W ( $10^{-4}$  m)

the wavefront tilt for a beam power of 100,000 watts. From Figure 6, the change in OPD from the center of the grid to the right-hand edge gives an estimated tilt of approximately 2 microradians. For a range of 1000 meters, this tilt causes a ray translation of 2 millimeters in the receiver plane. Compared to the untilted ray translations for this beam power, the tilt translation is small and can be ignored. However, the combination of higher beam powers and longer propagation ranges could produce a significant amount of translation.

#### Strehl Calculations

Since the variation in OPD for Figure 6 is large, the Strehl ratio for 100,000 watts will be very low. Thus, any imaging system looking at a grid area the same size as that of the high energy beam will be severely affected.

The effects of looking at smaller areas within the receiver plane proved to be very important. In general, the analysis showed that by looking at smaller areas within receiver plane, one could calculate a better Strehl ratio. Figure 7 is a comparison of Strehl ratios for a crosswind of 144 m/s. The Strehl ratios for a crosswind of 2.57 m/s were all zero and did not require plotting. Even for powers of 75,000 to 100,000 watts, the Strehl ratio is better when a receiver radius of 0.1 meters is used, and the ratio starts to fall off rapidly as the radius is increased. This

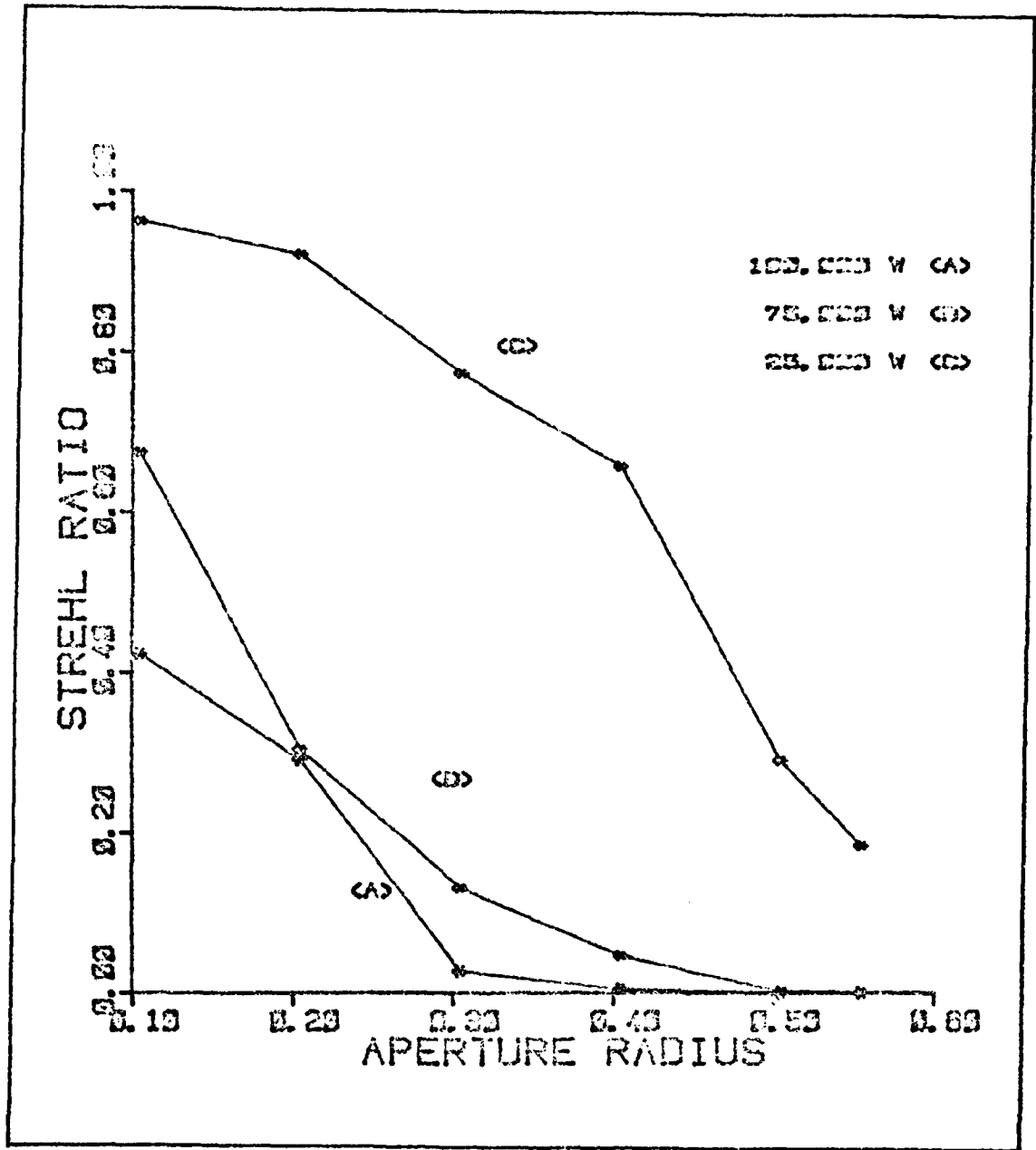


Figure 7. Strehl Ratio vs Aperture Radius

observation fits well when you consider Figure 6. Though there is a significant amount of OPD variation across the receiver plane, the variation over small portions of the plane are themselves small. However, it should be understood that limiting the aperture radius reduces the input signal. Thus, this reduced input signal can lead to a reduced signal-to-noise ratio and no significant improvement in the quality of a final image.

#### Location Of Blooming Effects

An attempt was made to determine which screen or screens contribute most to the reduction of the Strehl ratio. Figures 8, 9, and 10 are plots of the Strehl ratio when successive index screens are skipped or eliminated from the Strehl ratio calculation.

The plots reveal that the thermal blooming effects for higher beam powers are concentrated in the middle index planes (at 200 to 300 meters from the target plane). Index planes nearest the target have little effect on the Strehl ratio.

This observation does not appear to agree with published findings. It has been experimentally determined that blooming of a focused beam will reach its maximum somewhere near the focal plane (Ref 1:49). The value of "somewhere" is not strictly defined, so blooming in a plane

250 meters from the target might be feasible. However, one might expect the most severe blooming to occur closer to the focal (target) plane for a range of 1000 meters.

One explanation for the apparent disagreement in blooming locations is the fact that the launch angles of the rays from the target plane are small enough to keep the rays close together as they propagate through the first few index screens. Since all rays are launched from the same point in the target plane, they all see essentially the same index variation through the first few index screens. For this reason, the point at which thermal blooming effects begin to become noticeable is shifted away from the target plane.

Even if the rays are not kept close together, we would still expect to see the same type curves as those in Figure 8, 9, and 10. Once the high energy beam has been thermally bloomed, one might expect to see less significant changes in refractive index between that point and the target plane. Thus, those planes closest to the target plane would have little or no effect on the Strehl ratios.

However, it must be pointed out that the accuracy of this particular analysis is dependent upon the accuracy of the information determined in PROPMD. In certain situations, the spacing between index screens could greatly affect the resolution of index variations between these index screens. For beam powers greater than 100,000 watts, we would expect the point of maximum thermal blooming to

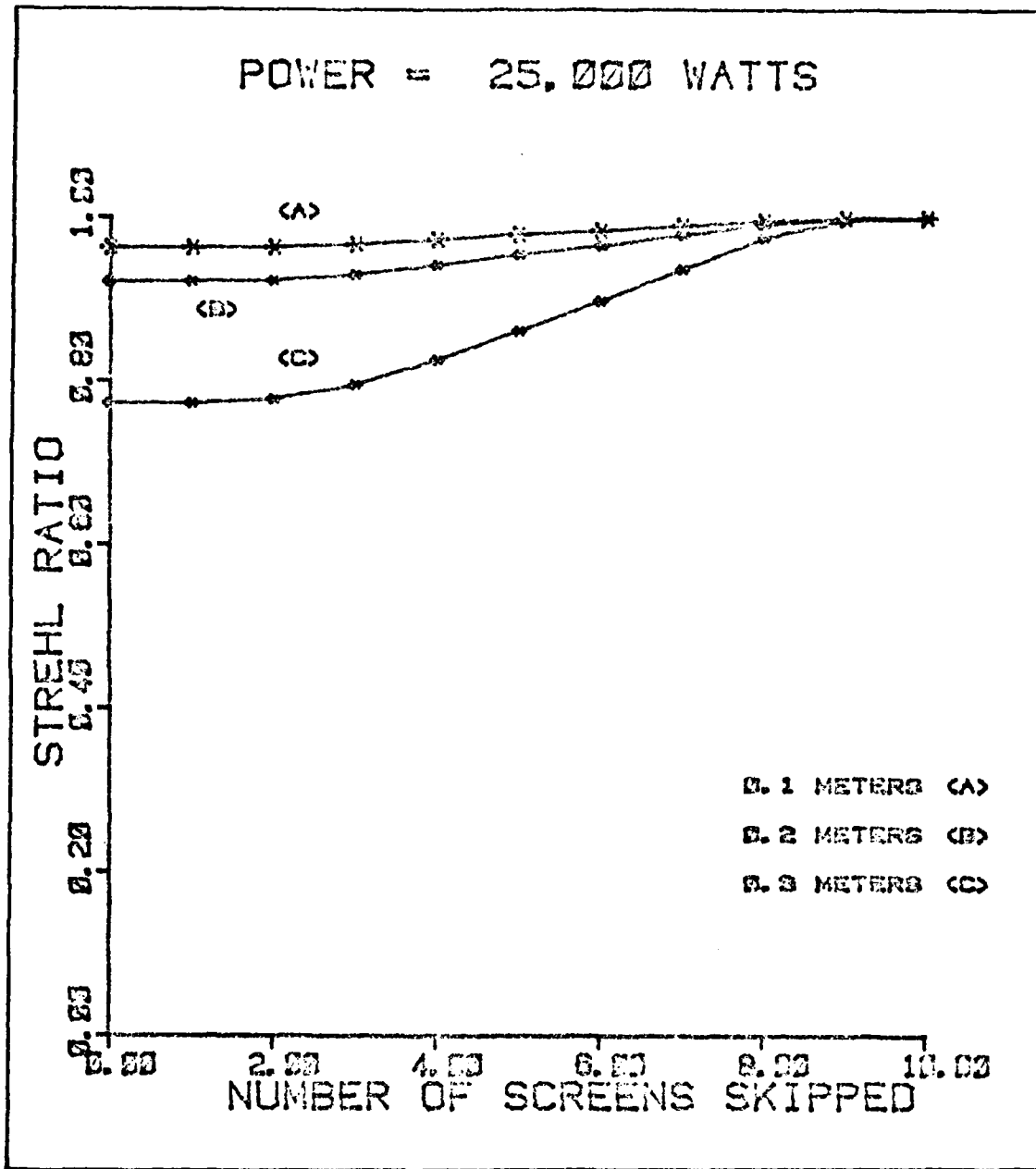


Figure 8. Strehl Ratio vs Screens Skipped (P=25,000 W)

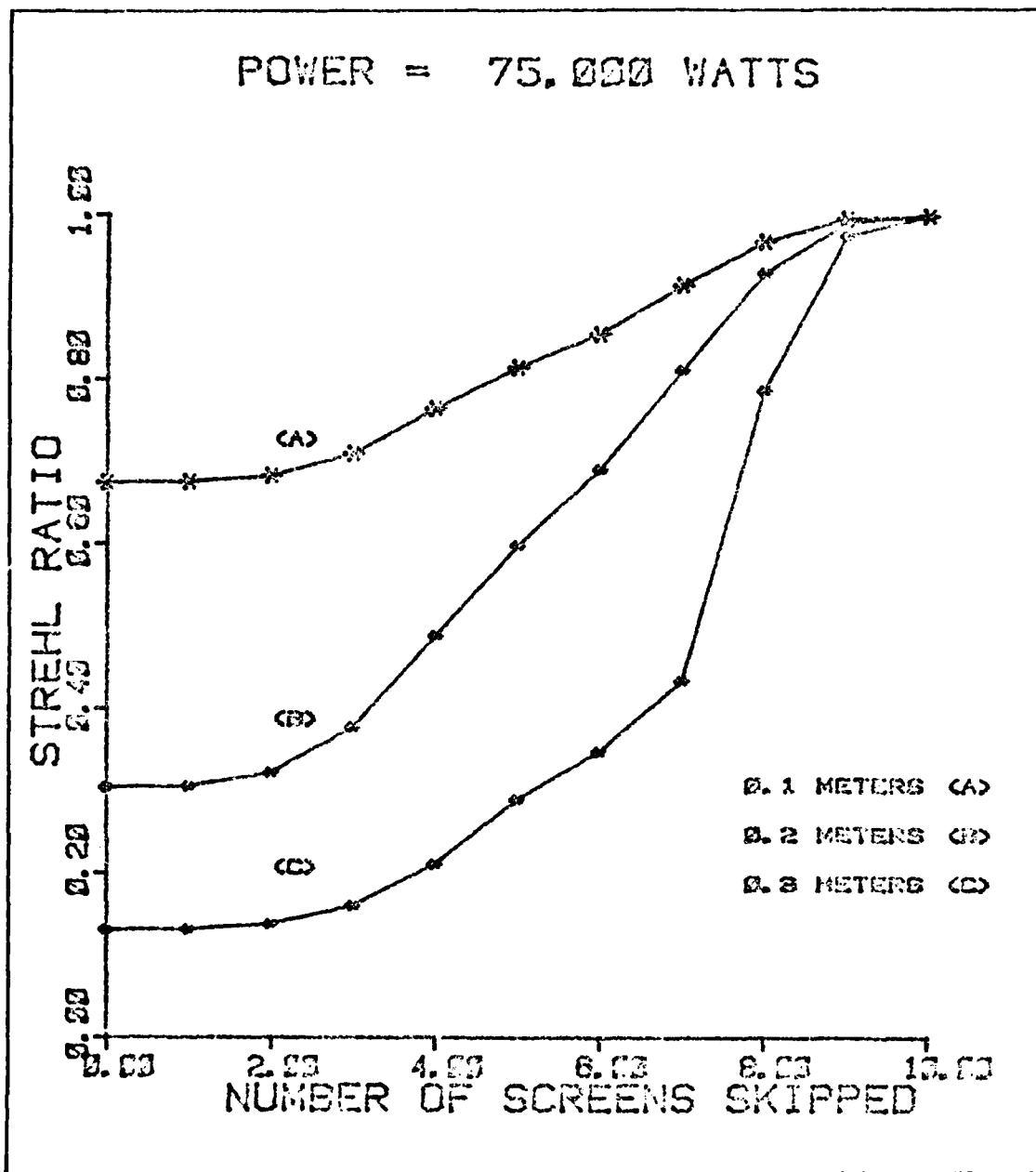


Figure 9. Strehl Ratio vs Screens Skipped (P=75,000 W)

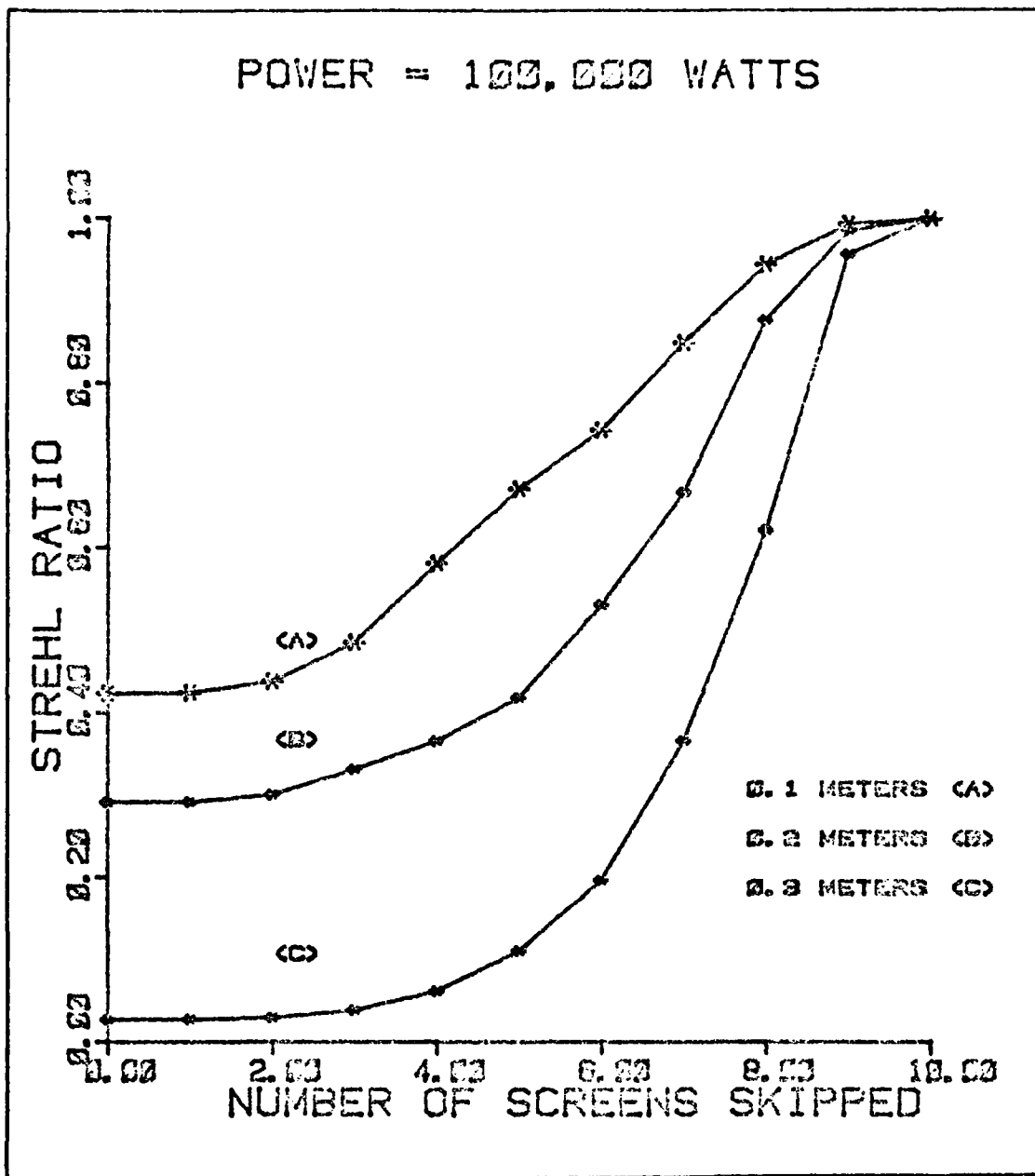


Figure 10. Strehl Ratio vs Screens Skipped (P=100,000 W)

shift farther away from the target plane. However, the PROPMD program spaces the planes according to the number of index screens requested. Thus, for higher beam powers, the maximum blooming could occur in areas where screen spacing is large.

## V CONCLUSIONS AND RECOMMENDATIONS

The objectives of this study were to:

a. Develop a computer code based on geometrical optics theory for propagating rays from a target plane to a receiver plane via a thermally bloomed medium.

b. Analyze the effects on the rays of propagation through a thermally bloomed medium.

Both of these objectives were met, and a listing of the developed computer code was included in Appendix C.

The analysis showed that for the combination of high beam powers and low crosswind speeds, the return wave in the plane of the receiver was degraded to the point that the Strehl ratio was always less than 0.1. Additionally, limiting the size of the receiver aperture did not improve the Strehl ratio no matter how small the aperture was.

For a crosswind of 144m/s, Strehl ratios could be improved by using smaller receiver apertures. However, one should be aware that tradeoffs must be made with respect to the resulting input signal reduction and possible reduction of the signal-to-noise ratio.

One significant result of this study was that ray refraction caused by thermal blooming was negligible. Thus, the rays were disturbed only with respect to their OPD values. However, there was a tilt in the returning wavefront. Since the propagating high energy beam was bent

into the wind, wavefronts traveling the same path were also bent. This bending caused returning wavefronts to be tilted with respect to the receiver plane.

Because light rays travel perpendicular to a wavefront, wavefront tilt implies that the light rays are bent. In this study, the affect of wavefront tilt on ray refraction was ignored, and an estimate on the amount of tilt for the 100,000 watt case was not considered large enough to invalidate the results of this study.

However, the effects of more significant amounts of tilt must be considered since the TRACE program does not accurately model the refraction of propagating rays. If this tilt is large enough in comparison with the original launch angle of an individual ray, then it can also have a significant effect on the OPD calculations. Even if the tilt is not significant at a range of 1000 meters and a beam power of 100,000 watts, it must be considered for different ranges and beam powers. Higher beam powers will cause more beam bending, and longer ranges will amplify the translation effects of tilt in the receiver plane.

Depending on the accuracy of the PROPMD calculations, the spacing of the index grid plane can have a significant effect on the resolution of index changes between grid points within an index plane. Therefore, in order to achieve the best possible resolution, the optimum grid spacing (optimum index array size) should be determined.

As a starting point, a linear interpolation scheme was used to determine the index variations between two index planes. Even though the process of thermal blooming is nonlinear in nature, a linear interpolation scheme is appropriate if PROPMD spaces the index screens properly. However, the results of determining the location of thermal blooming effects indicates that a higher order interpolation scheme would be more accurate.

Based on the above conclusions, the following recommendations are made:

1. The imaging optics should have the smallest field-of-view possible for the given minimum system requirements on input signal strength and signal-to-noise ratio.

2. Further study should be done at higher beam powers and longer ranges with effects of wavefront tilt included.

3. Further study should be done to determine the optimum grid spacing necessary for accurate resolution of index variations.

4. Investigation into the development of a higher order model for index variations between index planes should be made.

### Bibliography

1. Hogge, Charles B. Propagation of High-Energy Laser Beams in the Atmosphere. AFWL-TR-74-74. Kirtland AFB, New Mexico: Air Force Weapons Laboratory, June 1974.
2. Gebhardt, Frederick G. and David C. Smith. "Effects of Diffraction of the Self-induced Thermal Distortion of a Laser Beam in a Crosswind," Applied Optics, II, 244-248 (February 1972).
3. Hecht, Eugene and Alfred Zajac. Optics. Reading: Addison-Wesley Publishing Company, 1974.
4. Wang, J. Y. and D. E. Silva. "Wave-front Interpretation With Zernike Polynomials, " Applied Optics, 19 (9): 1510-1518 (May 1980).
5. Born, Max and Emil Wolf. Principles of Optics (Third edition). London: Pergamon Press, 1965.
6. Luneburg, R. K. Mathematical Theory of Optics. Los Angeles: University of California Press, 1964.

APPENDIX A

Luneburg's 3-D Refraction

APPENDIX A

Luneburg's 3-D Refraction (Ref 6:64-66)

The Luneburg 3-D refraction technique is generalized for any shaped surface of interface between two media of different refractive indices (see Figure 11).

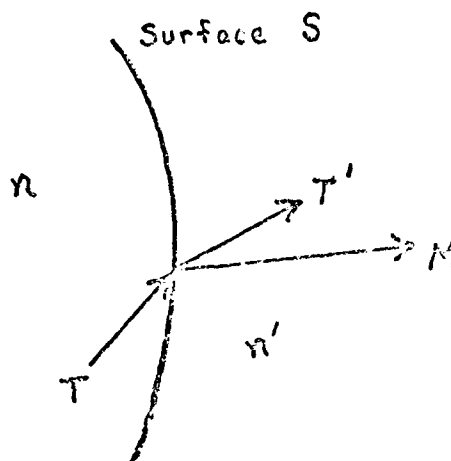


Figure 11. Geometrical Representation

M is a unit vector in the direction of the surface normal of S. T represents a unit vector in the direction of the incident ray, and T' is the unit vector of the refracted ray.

Luneburg's analysis develops the equation

$$n'T' - nT = \Gamma M \quad (8)$$

where  $\Gamma$  is a scale factor.

Since it is known that the refracted ray leaves the surface in a plane formed by the incident ray and the

surface normal  $M$ , it follows that the following vector equation is true

$$n'(T' \times M) = n(T \times M) \quad (9)$$

The lengths of the two vectors in equation 9 yield Snell's law

$$n' \sin \phi' = n \sin \phi \quad (10)$$

where

$\phi$  is the angle of incidence

$\phi'$  is the angle of refraction

The factor  $\Gamma$  is found by forming the scalar product

$$\Gamma = n'(T' \cdot M) - n(T \cdot M) \quad (11)$$

or

$$\Gamma = n' \cos \phi' - n \cos \phi \quad (12)$$

The equation of the surface normal  $M$  in this study is

$$M = 0 \hat{x} + 0 \hat{y} + 1 \hat{z} \quad (13)$$

Let

$$T = x_1 \hat{x} + y_1 \hat{y} + z_1 \hat{z} \quad (14)$$

and

$$T' = x_2 \hat{x} + y_2 \hat{y} + z_2 \hat{z} \quad (15)$$

Then equations 8, 13, 14, and 15 combine to give

$$\begin{aligned} n'(x_2 \hat{x} + y_2 \hat{y} + z_2 \hat{z}) - n(x_1 \hat{x} + y_1 \hat{y} + z_1 \hat{z}) \\ = (0 \hat{x} + 0 \hat{y} + 1 \hat{z}) \Gamma \quad (16) \end{aligned}$$

Equation 16 can be rearranged to yield

$$X_2 = (n/n') X_1 \quad (17)$$

$$Y_2 = (n/n') Y_1 \quad (18)$$

$$Z_2 = (\Gamma + n Z_1) / n' \quad (19)$$

Since T, T', and M are unit vectors,

$$T' \times M = \sin \phi' \quad (20)$$

$$T \times M = \sin \phi \quad (21)$$

Therefore, equation 9 gives

$$\phi' = \text{ARCSIN} \left[ (n/n') \sin \phi \right] \quad (22)$$

Combining equations 12 and 19 yields

$$Z_2 = (\Gamma + n Z_1) / n' = \cos \phi' \quad (23)$$

and the refracted unit vector T' is found.

APPENDIX B

PROPMD A Thermal Blooming Model

## APPENDIX B

### PROPMD A Thermal Blooming Model

PROPMD is a very sophisticated computer code written by Dr. Charles B. Hogge of the Air Force Weapons Laboratory. The program has been designed to allow great latitude in modeling the high-energy beam as well as the effects of atmospheric absorption and turbulence on the beam's propagation. PROPMD can simulate the firing of a laser beam from either a stationary or moving platform. A crosswind at any speed and at any angle with respect to the beam propagation path can be selected, and the beam itself can travel at any angle with respect to horizontal (i.e. an airborne platform with the beam aimed downward and to the rear of the aircraft). There are input parameters that can simulate a particular atmospheric turbulence situation. The beam characteristics (power, wavelength, beam size, pulse length, etc.) are input along with appropriate values of the absorption coefficients and relaxation times for carbon dioxide (CO<sub>2</sub>) and water in order to model the absorption of the beam, particularly the CO<sub>2</sub> laser beam of wavelength 10.6 micrometers.

The actual location of phase (index) screens can either be input by the user or left to the program to calculate internally depending on how many screens are requested. For 5 and 10 screens, the internally generated spacings are as

shown in Figure 12. Since the thermal blooming has its greatest effect near the target plane, the screens are necessarily close together in that area of the propagation path.

One important feature internal to the program is its compression of the x-y grid as the beam propagates toward the target. The overall grid size of the propagating beam is reduced to simulate focusing of the beam. Consequently, the spacing between index array elements is reduced.

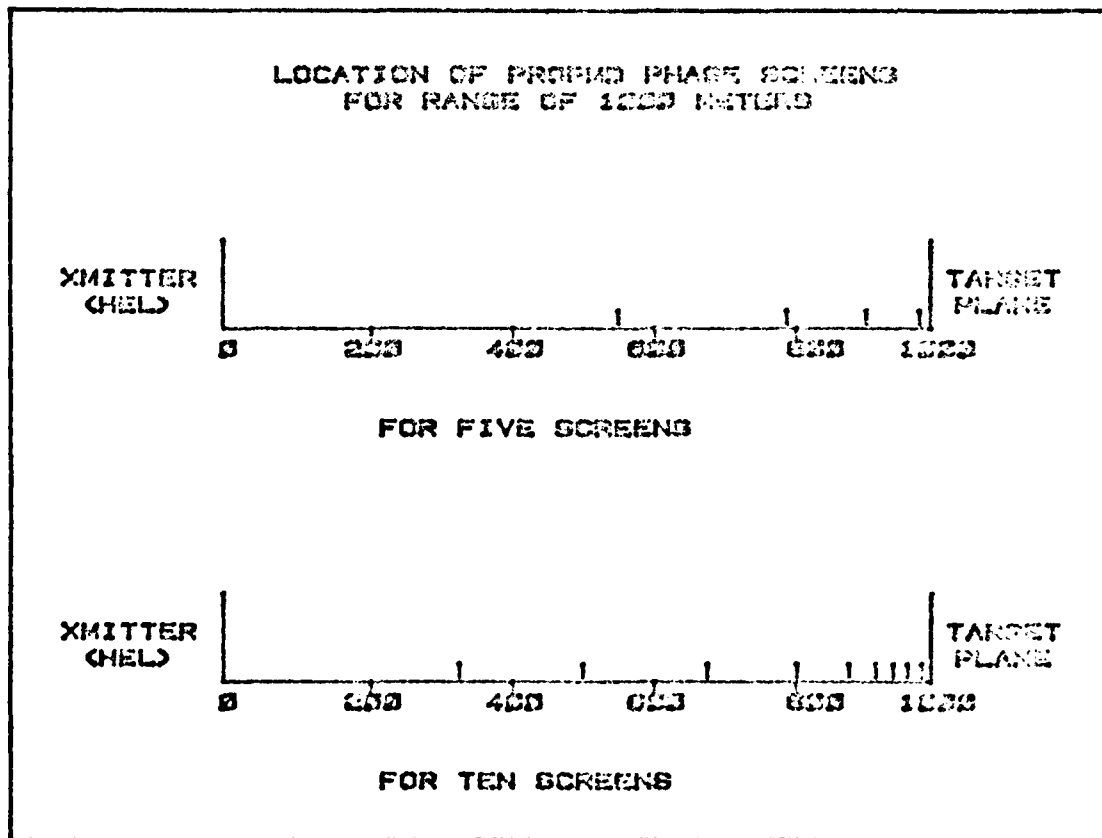


Figure 12. Phase Screen Locations In PROPPMD

The determination of thermal blooming effects at each screen is actually a calculation of phase perturbations across the beam grid. These perturbations are directly related to the refractive index  $n$  and can be easily converted.

For persons who wish to use PROPMD in conjunction with TRACE, the following additions to PROPMD are needed:

1. In the program card of DEVICE, TAPE22 should be added.

2. After line 131 of DEVICE, add:

```
WRITE(22) CITOT, WAVE, RANGE, PETAM, NSTP(1)
```

3. After line 97 of PROPMD, add:

```
DXPX = PX(2) - PX(1)  
WRITE(22) DXPX, NLM
```

4. After line 995 of PROPMD, add:

```
WRITE(22) K, AZ
```

5. After line 49 of CWTM, add:

```
DXPX = PX(2) - PX(1)  
WRITE(22) DXPX  
DO 969 II=1, NLM  
969 WRITE(22) (UUS(II,JJ),JJ=1,NLM)
```

After a successful run of PROPMD, the data written on tape 22 must still be manipulated. The data is oriented to propagation towards the target. Whereas, the ray trace is away from the target. Thus, the order of the screens must be reversed.

In addition, the following sample operation must be performed on each screen's array (see DATA in Appendix C):

```
DO 100 I = 1, NLM
A(I,1) = 1. + PETAM
DO 100 J = 2, NLM
A(I,J) = A(I,J)/(2PI/WAVE) + (1. + PETAM)
100 CONTINUE
```

where  $2\text{PI} = 6.28318$ .

Using the values of RANGE and AZ, the spacing between screens can be calculated.

The following is a list of sample PROPMD input parameters used in this study:

CITOT	=	.1 E-6	RADIN	=	0.
WAVE	=	.106 E-4	RADOUT	=	0.29 E+0
VEL	=	.144 E+3	BEAMSZ	=	.29 E+1
RANGE	=	.1 E+4	BETA	=	.2 E+1
FL	=	.1 E+4	TURBCST	=	.1 E-23
PALPWAT	=	.19 E-4	GRNDLEV	=	.54 E+4
PALPCO2	=	.627 E-4	RATE	=	.1 E+1
PTAU	=	.85 E-5	TPULSE	=	.1 E+1
PETAM	=	.272 E-3	ADAP	=	.1 E+1
PPO	=	.1013 E+4	NRSS	=	1
AZANGLE	=	-.9 E+2	NSTPSIZ	=	0
ELANGLE	=	0.	GAREO	=	0. , 0.
TMSDFLT	=	.1 E+1	PSCAT	=	.1 E-13
RATIO	=	.1 E+1	RHO	=	0.
COORUPD	=	.15 E+0	BLOSS	=	.1 E+1
THETAJ	=	0.	SOASP	=	0.



APPENDIX C

Source Listings for TRACE and DATA







\*\*\*\*\*

◆ DO LOOP TO PROPAGATE ALL RAYS THRU DELTA Z INCREMENT

\*\*\*\*\*

```
100 CONTINUE
   TO 500 I=1,NRAY
   ANGLE(I)=RAY(I,7)
   IF (DEL.LE.0.0001) GO TO 110
   IF (RAY(I,7).LT.0.) GO TO 500
```

\*\*\*\*\*

◆ FIND ANGLE OF INCIDENCE

\*\*\*\*\*

```
CALL ANGLE(RAY(I,5),THETA)
```

\*\*\*\*\*

◆ FIND X & Y COORDINATES AT NEW MIDPLANE

\*\*\*\*\*

```
XLAST = RAY(I,1)
YLAST = RAY(I,3)
```

```
CALL XYNEW(RAY(I,1),RAY(I,2),RAY(I,3),RAY(I,4),ZPLAST,
$ZPNEM,RAY(I,5),RAY(I,1),RAY(I,3))
```

\*\*\*\*\*

◆ AT THIS POINT WE MUST INTERPOLATE NEW N(X,Y)

\*\*\*\*\*

```
110 CONTINUE
   IF (I.GT.1) GO TO 130
   READ(21) NPLANE, DELZY
   DO 120 II=1,NLM
120  READ(21) (RINDEX(II,JJ),JJ=1,NLM)
130  CONTINUE
   CALL ANDEX(DELZY,RAY(I,1),RAY(I,3),NLM,RAY(I,7),
$  RINDEX,XX,YY,I)
   IF (RAY(I,7).GT.0.) GO TO 140
```

\*\*\*\*\*

- ◆ IF THE INDEX IS FOUND TO BE NEGATIVE, THE RAY IS OFF THE
- ◆ GRID AND NO MORE CALCULATIONS ARE NEEDED FOR THIS RAY.

\*\*\*\*\*

NPLAN(I) = NPLANE  
GO TO 500  
140 CONTINUE

- ◆ IF NFLAG IS SET, THEN NFLAG - 1 SCREENS WILL BE SKIPPED IN
- ◆ THE RAY TRACE BEFORE REFRACTION AND OPD CALCS ARE MADE

IF (NFLAG.GE.K) ANLAST(I) = RAY(I,7)

IF (DELZ.LE.0.0001) GO TO 500

\*\*\*\*\*

- ◆ FIND AVERAGE INDEX BETWEEN MIDPLANES

\*\*\*\*\*

CALL AVGN(ANLAST(I), RAY(I,7), ANBAR(I))

\*\*\*\*\*

- ◆ FIND THE OPD BETWEEN MIDPLANES

\*\*\*\*\*

IF (K.LE.NFLAG) ANBAR(I) = NZERO  
CALL DPL(RAY(I,6), XLAST, RAY(I,1), YLAST, RAY(I,3), ZPLAST, ZPNEW,  
& ANBAR(I))

- ◆ BRING THE OPD CALCULATION UP-TO-DATE

X=RAY(I,1)

Y=RAY(I,3)

\*\*\*\*\*

- ◆ FIND REFRACTION ANGLE AND NEW DIRECTION COSINES

\*\*\*\*\*





```

505 FORMAT(4X, * FOR RAY*, I3//)
WRITE(6,506) XD(I), ALPX(I), RAY(I,1), RAY(I,2)
WRITE(6,507) YD(I), ALPY(I), RAY(I,3), RAY(I,4)
WRITE(6,508) RAY(I,5)
506 FORMAT(2X, * XD =*, G18.12, 4X, * ALPHA XD =*, G18.12, 4X
$, * Y =*, G18.12, 6X, * ALPHA YF =*, G18.12//)
507 FORMAT(2X, * YD =*, G18.12, 4X, * ALPHA YD =*, G18.12, 4X
$, * YF =*, G18.12, 6X, * ALPHA YF =*, G18.12//)
508 FORMAT(3X, * ALPHA ZF =*, G18.12//)
WRITE(6,509) RAY(I,7)
509 FORMAT(27X, * THE FINAL INDEX OF REFRACTION IS **, G18.12//)
WRITE(6,510) OPDIFF(I)
510 FORMAT(67X, * THE TOTAL OPTICAL PATH DIFFERENCE IS **, G18.12//)
GO TO 8000
7000 IF(NPLAN(I).EQ.1) GO TO 7100
NPMINUS = NPLAN(I) - 1
WRITE(6,511) XD(I), ALPX(I), NPMINUS, NPLAN(I)
511 FORMAT(8X, * XD =*, G18.12, 4X, * ALPHA XD =*, G18.12, 4X
$, * THE RAY LEFT THE BEAM GRID BETWEEN PLANES **, I3, * AND **, I3, * .*)
WRITE(6,512) YD(I), ALPY(I)
512 FORMAT(8X, * YD =*, G18.12, 4X, * ALPHA YD =*, G18.12//)
GO TO 8000
7100 CONTINUE
WRITE(6,513) XD(I), ALPX(I), NPLAN(I)
513 FORMAT(8X, * XD =*, G18.12, 4X, * ALPHA XD =*, G18.12, 4X
$, * THE RAY LEFT THE BEAM GRID BETWEEN THE TARGET PLANE AND PLANE **, I3
$, * .*)
WRITE(6,514) YD(I), ALPY(I)
514 FORMAT(8X, * YD =*, G18.12, 4X, * ALPHA YD =*, G18.12//)
8000 CONTINUE
8050 WRITE(6,515) DIFF, ASDPD, SROPD, STREHL
515 FORMAT(25X, * THE MAXIMUM DEVIATION ACROSS THE OUTPUT PLANE IS **,
$, G18.12//, 25X, * OPDSQBAR =*, G18.12, 6X, * OPDBARSD =*, G18.12//, 25X,
$, * THE STREHL RATIO FOR THIS RUN IS **, G18.8//)
IF(MASK.EQ.20) WRITE(6,516)
516 FORMAT(25X, *-----NOTE: THIS STREHL RATIO IS MASKED TO 0.2
$, METERS.-----//)
IF(MASK.EQ.30) WRITE(6,517)
IF(MASK.EQ.10) WRITE(6,518)
517 FORMAT(25X, *-----NOTE: THIS STREHL RATIO IS MASKED TO 0.3
$, METERS.-----//)
IF(MASK.EQ.40) WRITE(6,522)
522 FORMAT(25X, *-----NOTE: THIS STREHL RATIO IS MASKED TO 0.4
$, METERS.-----//)
IF(MASK.EQ.50) WRITE(6,523)
523 FORMAT(25X, *-----NOTE: THIS STREHL RATIO IS MASKED TO 0.5
$, METERS.-----//)
IF(MASK.EQ.55) WRITE(6,524)
524 FORMAT(25X, *-----NOTE: THIS STREHL RATIO IS MASKED TO 0.55
$, METERS.-----//)

```



```

*****
SUBROUTINE OPL(OPD,XOLD,XNEW,YOLD,YNEW,ZOLD,ZNEW,C1,AP)
  ◆ CALCULATE OPTICAL PATH LENGTH BETWEEN MIDPLANES
  DELX = XNEW - XOLD
  DELY = YNEW - YOLD
  DELZ = ZNEW - ZOLD
  R = SQRT(DELX*DELX + DELY*DELY + DELZ*DELZ)
  OPD = OPD + ANPR*R
  RETURN
END

```

```

*****
SUBROUTINE CPPP(ZSOLD,ZSHU,DELZHM,ZPNU)
  ◆ FIND NEW LOCATIONS OF PHASE SCREENS AND THEIR
  ◆ RESPECTIVE MIDPLANES
  ZPNU = ZSOLD + (DELZHM)/2
  ZSHU = ZSOLD + DELZHM
  RETURN
END

```

```

*****
SUBROUTINE ANGLE(TZIN,THETA)
  ◆ FIND ANGLE OF RAY TO SURFACE NORMAL
  ◆ TZIN = DIRECTION COSINE OF RAY WITH Z AXIS
  THETA=ACOS(TZIN)
  RETURN
END

```

```

*****
SUBROUTINE REUNITV(TXIN,TYIN,TZIN,ANIN,ANRF,THETAR)
  ◆ FIND UNIT VECTOR OF THE REFRACTED RAY

  ◆ TXIN, TYIN, & TZIN ARE DIRECTION COSINES OF INCIDENT RAY
  ◆ ON INPUT AND THE DIRECTION COSINES OF THE REFRACTED RAY
  ◆ ON OUTPUT

  ◆ ANIN (ANRF) IS THE INDEX OF THE INCIDENT (REFRACTED) RAY
  ◆ THETAR = REFRACTION ANGLE
  THETAR=ASIN((ANIN/ANRF)*SIN(THETAR))
  TXIN=(ANIN/ANRF)*TXIN
  TYIN=(ANIN/ANRF)*TYIN
  TZIN=COS(THETAR)
  RETURN
END

```



```
Y(I) = (NL2-I)*DELXY + DELXY2
99 X(I) = (NL2-I)*DELX + DELX2
100 CONTINUE
```

\*\*\*\*\*

◆ CHECK TO SEE IF EITHER COORDINATE IS OUTSIDE GRID

\*\*\*\*\*

```
IF (XRAY.GT.X(NL)) GO TO 200
IF (XRAY.LT.X(NL)) GO TO 200
IF (YRAY.GT.Y(I)) GO TO 200
IF (YRAY.LT.Y(NL)) GO TO 200
```

\*\*\*\*\*

◆ INTERPOLATING FOR X GRID VALUE

\*\*\*\*\*

```
DO 120 I=2,NL
IF (XRAY.LT.X(I)) GO TO 120
IXH = I-1
IXL = I
GO TO 130
120 CONTINUE
```

\*\*\*\*\*

◆ NOW LOOKING FOR THE Y GRID VALUE

\*\*\*\*\*

```
130 DO 140 I =2,NL
IF (YRAY.LT.Y(I)) GO TO 140
IYL = I
IYH = I - 1
GO TO 150
140 CONTINUE
```

\*\*\*\*\*

◆ INTERPOLATING FOR AN INDEX VALUE LOCATED  
◆ INSIDE THE BOX OF FOUR MATRIX VALUES

\*\*\*\*\*

```

150 XP = XRAY - X(IXL)
    YO = YRAY - Y(IYL)
    ENDEXL = AINDEX(IYL, IXL) + ((AINDEX(IYL, IXH) - AINDEX(IYL, IXL)) /
$DELX) * XP
    ENDEXH = AINDEX(IYH, IXL) + ((AINDEX(IYH, IXH) - AINDEX(IYH, IXL)) /
$DELX) * XP
    ENDEXF = ENDEXL + (ENDEXH - ENDEXL) / DELX * YO
    RETURN
200 CONTINUE
    * RAY COORDINATES ARE OUTSIDE GRIDBOUNDS--SET INDEX NEGATIVE.
    ENDEXF = -900.
    RETURN
    END

```

```

PROGRAM DATA(INPUT,OUTPUT,TAPE22,TAPE21)
DIMENSION NPLANE(11),DELZ(11),A(64,64),B(64,64),C(64,64)
DIMENSION D(64,64),E(64,64),F(64,64), DELXY(11), DELTAC(11)
DIMENSION G(64,64),H(64,64),R(64,64),S(64,64),T(64,64)
READ(22) POWER, WAVE, RANGE, PETAM, NDZ
READ(22) DELXY(1), NLM
READ(22) NPLANE(1), DELZ(1)
CFBS = 2*3.14159/WAVE
DO 99 I=1,NLM
DO 98 J=1,NLM
98 T(I,J) = 1.0 + PETAM
99 CONTINUE
READ(22) DELXY(2)
DO 5 I=1,NLM
5 READ(22) (C(I,J),J=1,NLM)
READ(22) NPLANE(2), DELZ(2)
READ(22) DELXY(3)
DO 6 I=1,NLM
6 READ(22) (P(I,J),J=1,NLM)
READ(22) NPLANE(3), DELZ(3)
READ(22) DELXY(4)
DO 7 I=1,NLM
7 READ(22) (H(I,J),J=1,NLM)
READ(22) NPLANE(4), DELZ(4)
READ(22) DELXY(5)
DO 8 I=1,NLM
8 READ(22) (G(I,J),J=1,NLM)
READ(22) NPLANE(5), DELZ(5)
READ(22) DELXY(6)
DO 9 I=1,NLM
9 READ(22) (F(I,J),J=1,NLM)
READ(22) NPLANE(6), DELZ(6)
READ(22) DELXY(7)
DO 10 I=1,NLM
10 READ(22) (E(I,J),J=1,NLM)
READ(22) NPLANE(7), DELZ(7)
READ(22) DELXY(8)
DO 11 I=1,NLM
11 READ(22) (D(I,J),J=1,NLM)
READ(22) NPLANE(8), DELZ(8)
READ(22) DELXY(9)
DO 12 I=1,NLM
12 READ(22) (C(I,J),J=1,NLM)
READ(22) NPLANE(9), DELZ(9)
READ(22) DELXY(10)
DO 13 I=1,NLM
13 READ(22) (B(I,J),J=1,NLM)
READ(22) NPLANE(10), DELZ(10)
READ(22) DELXY(11)
DO 14 I=1,NLM

```

```

14 READ(22) (A(I,J),J=1,NLM)
   READ(22) NPLANE(11), DELZ(11)
   RANGE = RANGE
   DO 19 I=1,11
   DELTAZ(I) = RANGE - DELZ(12-I)
   RANGE = DELZ(12-I)
   IF(I.EQ.11) GO TO 16
15 CONTINUE
16 CONTINUE
   DO 22 I=1,NLM
   A(I,1) = 0.
   B(I,1) = 0.
   C(I,1) = 0.
   D(I,1) = 0.
   E(I,1) = 0.
   F(I,1) = 0.
   G(I,1) = 0.
   H(I,1) = 0.
   R(I,1) = 0.
   S(I,1) = 0.
   DO 21 J=1,NLM
   A(I,J) = A(I,J)/CKDEX + T(I,J)
   B(I,J) = B(I,J)/CKDEX + T(I,J)
   C(I,J) = C(I,J)/CKDEX + T(I,J)
   D(I,J) = D(I,J)/CKDEX + T(I,J)
   E(I,J) = E(I,J)/CKDEX + T(I,J)
   F(I,J) = F(I,J)/CKDEX + T(I,J)
   G(I,J) = G(I,J)/CKDEX + T(I,J)
   H(I,J) = H(I,J)/CKDEX + T(I,J)
   R(I,J) = R(I,J)/CKDEX + T(I,J)
21 S(I,J) = S(I,J)/CKDEX + T(I,J)
22 CONTINUE
   WRITE(21) POWER, WAVE, RANGE, PETAM
     * FIRST PLANE IS TARGET PLANE
   WRITE(21) NDZ, NLM
   WRITE(21) DELTAZ(1)
   WRITE(21) NPLANE(1), DELXY(11)
   DO 31 I=1,NLM
31 WRITE(21) (A(I,J),J=1,NLM)
   WRITE(21) DELTAZ(2)
   WRITE(21) NPLANE(2), DELXY(10)
   DO 32 I=1,NLM
32 WRITE(21) (B(I,J),J=1,NLM)
   WRITE(21) DELTAZ(3)
   WRITE(21) NPLANE(3), DELXY(9)
   DO 33 I=1,NLM
33 WRITE(21) (C(I,J),J=1,NLM)
   WRITE(21) DELTAZ(4)

```

```

WRITE (21) NPLANE (4), DELXY (8)
DO 34 I=1,NLM
34 WRITE (21) (D(I,J),J=1,NLM)
WRITE (21) DELTAZ (5)
WRITE (21) NPLANE (5), DELXY (7)
DO 35 I=1,NLM
35 WRITE (21) (E(I,J),J=1,NLM)
WRITE (21) DELTAZ (6)
WRITE (21) NPLANE (6), DELXY (6)
DO 36 I=1,NLM
36 WRITE (21) (F(I,J),J=1,NLM)
WRITE (21) DELTAZ (7)
WRITE (21) NPLANE (7), DELXY (5)
DO 37 I=1,NLM
37 WRITE (21) (G(I,J),J=1,NLM)
WRITE (21) DELTAZ (8)
WRITE (21) NPLANE (8), DELXY (4)
DO 38 I=1,NLM
38 WRITE (21) (H(I,J),J=1,NLM)
WRITE (21) DELTAZ (9)
WRITE (21) NPLANE (9), DELXY (3)
DO 39 I=1,NLM
39 WRITE (21) (R(I,J),J=1,NLM)
WRITE (21) DELTAZ (10)
WRITE (21) NPLANE (10), DELXY (2)
DO 40 I=1,NLM
40 WRITE (21) (S(I,J),J=1,NLM)
WRITE (21) DELTAZ (11)
WRITE (21) NPLANE (11), DELXY (1)
DO 41 I=1,NLM
41 WRITE (21) (T(I,J),J=1,NLM)
PRINT*, " "
PRINT*, POWER, WAVE, RANGE
PRINT*, " "
PRINT*, (A(32,J),J=1,10)
ENDFILE 21
STOP
END

```

## VITA

Michael Thomas Baker was born on 25 June 1948 in Greensboro, North Carolina. He graduated from high school in Burlington, North Carolina in 1966 and attended North Carolina State University for two years. In 1968, he enlisted in the United States Air Force where he served as a telecommunications systems control specialist. He left the Air Force as a staff sergeant in 1973 and reentered North Carolina State University, from which he received the degree of Bachelor of Science in Electrical Engineering in August 1976. While attending North Carolina State University, he was a member of the Air Force Reserve Officer Training Corps from which he received his Commission in December 1976. His first assignment was to Sacramento Air Logistics Center at McClellan AFB, California in February 1977 as a communications systems engineer, and he remained there until entering the School of Engineering, Air Force Institute of Technology, in June 1979.

Permanent address: 3327 Arapaho Way  
North Highlands, California 95660

Unclassified

SECURITY CLASSIFICATION OF THIS PAGE (When Data Entered)

REPORT DOCUMENTATION PAGE		READ INSTRUCTIONS BEFORE COMPLETING FORM
1. REPORT NUMBER AFIT/RNO/PH/80-2	2. GOVT ACCESSION NO. AD-A094721	3. RECIPIENT'S CATALOG NUMBER
4. TITLE (and Subtitle)  RETURN WAVE ANALYSIS IN A THERMALLY BLOOMED MEDIUM	5. TYPE OF REPORT & PERIOD COVERED MS Thesis	
	6. PERFORMING ORG. REPORT NUMBER	
7. AUTHOR(s) Michael T. Baker 1st Lt USAF	8. CONTRACT OR GRANT NUMBER(s)	
9. PERFORMING ORGANIZATION NAME AND ADDRESS Air Force Institute of Technology (AFIT-ET) Wright Patterson AFB, Ohio 45433	10. PROGRAM ELEMENT, PROJECT, TASK AREA & WORK UNIT NUMBERS	
11. CONTROLLING OFFICE NAME AND ADDRESS Air Force Weapons Laboratory (AWL-AR) Kirtland AFB, New Mexico 87185	12. REPORT DATE December 1980	
	13. NUMBER OF PAGES 66	
14. MONITORING AGENCY NAME & ADDRESS (if different from Controlling Office)	15. SECURITY CLASS. (of this report) Unclassified	
	15a. DECLASSIFICATION DOWNGRADING SCHEDULE	
16. DISTRIBUTION STATEMENT (of this Report)  Approved for public release; distribution unlimited		
17. DISTRIBUTION STATEMENT (of the abstract entered in Block 20, if different from Report)		
18. SUPPLEMENTARY NOTES Approved for public release; IAW AFR 190-17  Frederick C. Lynch, Major, USAF Director of Public Affairs		
19. KEY WORDS (Continue on reverse side if necessary and identify by block number) Ray Trace Imaging Thermal Blooming		
20. ABSTRACT (Continue on reverse side if necessary and identify by block number) A computer code was developed to perform a geometrical ray trace of a light ray from a target plane to a receiver plane via a thermally bloomed medium. Thermal blooming was modeled using a computer code from the Air Force Weapons Laboratory called FPOEM.  Ray traces were done for various degrees of thermal blooming, and Strehl ratios were made for each situation. Also, contour plots of the		

DD FORM 1473 1 JAN 73

EDITION OF 1 NOV 65 IS OBSOLETE

Unclassified

SECURITY CLASSIFICATION OF THIS PAGE (When Data Entered)

→ ray optical path deviations across the receiver plane were made.

Results showed that a ray's direction of propagation was virtually unaffected by refraction. Disturbance of the ray was due totally to the effect of thermal blooming on the optical path length of the ray. In severe blooming situations, calculated Strehl ratios were less than 0.1. However, limiting the size of the receiver optics to something less than the size of the high-energy beam grid led to improved Strehl ratios.

Unclassified

**LMED**  
**8**